

# Visual Binaries in the Orion Nebula Cluster

Bo Reipurth<sup>1</sup>, Marcelo M. Guimarães<sup>1,2</sup>, Michael S. Connelley<sup>1,3</sup>, and John Bally<sup>4</sup>

## ABSTRACT

We have carried out a major survey for visual binaries towards the Orion Nebula Cluster using HST images obtained with an H $\alpha$  filter. Among 781 likely ONC members more than 60'' from  $\theta^1$  Ori C, we find 78 multiple systems (75 binaries and 3 triples), of which 55 are new discoveries, in the range from 0''.1 to 1''.5. About 9 binaries are likely line-of-sight associations. We find a binary fraction of  $8.8\% \pm 1.1\%$  within the limited separation range from 67.5 to 675 AU. The field binary fraction in the same range is a factor 1.5 higher. Within the range 150 AU to 675 AU we find that T Tauri associations have a factor 2.2 more binaries than the ONC. The binary separation distribution function of the ONC shows unusual structure, with a sudden steep decrease in the number of binaries as the separation increases beyond 0''.5, corresponding to 225 AU. We have measured the ratio of binaries wider than 0''.5 to binaries closer than 0''.5 as a function of distance from the Trapezium, and find that this ratio is significantly depressed in the inner region of the ONC. The deficit of wide binaries in the central part of the cluster is likely due to dissolution or orbital change during their passage through the potential well of the inner cluster region. Many of the companions are likely to be brown dwarfs.

*Subject headings:* binaries: visual — stars: pre-main sequence — stars: low-mass, brown dwarfs — open clusters and associations: individual(Orion Nebula Cluster) — techniques: high angular resolution

## 1. INTRODUCTION

Since the first detection of pre-main sequence binaries by Joy & van Biesbroeck (1944) and Herbig (1962), major advances have been gained in our understanding of the formation and early evolution of binaries. One of the key results is that binaries are about twice as common in T Tauri associations as among field stars (e.g., Reipurth & Zinnecker 1993, Simon et al. 1995, Duchêne 1999, Ratzka et al. 2005). Studies of embedded sources suggest that multiple systems may possibly be more prevalent among Class I sources than among the more evolved T Tauri stars (e.g., Duchêne et al. 2004). Dynamical evolution among higher-order multiples is likely to be important during the

embedded phase, leading to the occasional ejection of lower-mass members and the formation of powerful jets (Reipurth 2000).

The Orion Nebula Cluster (ONC) is the nearest ( $d \sim 450$  pc) star forming cluster, with an age of less than 1 Myr, and it has been extensively studied at multiple wavelengths (e.g., Herbig & Terndrup 1986, Hillenbrand 1997, Getman et al. 2005 and references therein; for earlier work see the review by Herbig 1982). It is well known that the massive stars in the Trapezium have a very high binary frequency (e.g., Preibisch et al. 1999). Binarity of the low-mass population of the central part of the ONC has been studied extensively, and it has been suggested that the binary frequency is lower than for the dispersed low-mass young population in associations and comparable to the binary frequency in the field (Prosser et al. 1994, Padgett et al. 1997, Petr et al. 1998, Simon et al. 1999, Köhler et al. 2006).

In this paper, we report the results of a major binary survey of an extensive region centered on

<sup>1</sup>Institute for Astronomy, University of Hawaii, 640 N. Aohoku Place, Hilo, HI 96720 (reipurth@ifh.hawaii.edu)

<sup>2</sup>Departamento de Física, UFMG, Caixa Postal 702, 30.123-970, Belo Horizonte, MG, Brazil

<sup>3</sup>NASA Ames Research Center, Moffett Field, CA 94035

<sup>4</sup>CASA, University of Colorado, 389 UCB, Boulder, Colorado 80309-0389

the ONC, based on a large H $\alpha$  imaging survey using the Hubble Space Telescope. We have detected 78 multiple systems, of which 55 are new discoveries, in an area of 412 arcmin<sup>2</sup> that excludes a circular area with radius of 60'' centered on  $\theta^1$  Ori C. We discuss the membership of these binaries in the ONC, analyze their binary properties, and discuss the binary separation distribution function and binary formation in the ONC.

## 2. OBSERVATIONS

The present survey is based on our recent study of the Orion Nebula using the Wide Field Camera of the Advanced Camera for Surveys onboard HST. During program GO-9825, we observed 26 ACS fields with the F658N (H $\alpha$ + [NII]) filter and with an exposure time of 500 sec per pointing. In total our H $\alpha$  survey covers an area of 415 arcmin<sup>2</sup> of the central Orion Nebula. Due to the high stellar density near the Trapezium we have excluded a circular area with radius of 60'' centered on  $\theta^1$  Ori C, so the area investigated is 412 arcmin<sup>2</sup>. The exquisite resolution of the HST combined with the 0''.05 pixel-size of the ACS offers a unique opportunity to detect close binaries. We examined all stellar sources in the images by eye at a range of contrast levels, allowing us to pick up faint as well as bright companions. Thanks to the very stable point-spread function across the images, this could be done in a rather homogeneous fashion. We discuss the completeness of this procedure in Sect. 3.3. We used reduced images that were combined through MULTIDRIZZLE. The faintest star we measured had a magnitude of 21.5 in the F658 filter. Pixel coordinates for both primaries and secondaries were determined with 2-dimensional Gaussian functions, and separations and position angles calculated from these coordinates. Relative fluxes were determined using aperture photometry with corrections for the sky background. For further details of the observations, see Bally et al. (2006).

## 3. SELECTION OF SAMPLE

### 3.1. Survey Area

The region of the ONC we have studied is shown in Figure 1, which outlines the mosaic of 26 ACS fields. One field had to be slightly turned to

acquire a guidestar. We examined all stars (1051) in these fields with the exception of stars within an exclusion zone of 60'' around  $\theta^1$  Ori C.

### 3.2. Separation Limits

All previous HST studies of binarity in the ONC were done in the region around the Trapezium, where line-of-sight pairs due to the high stellar density is a major issue, and thus focused mostly on sub-arcsec binaries. In contrast, our study covers a much larger area including the outskirts of the ONC. We have also excluded the inner region with radius of 60'', so contamination is much less of an issue. Based on our observed star density, we can calculate the fraction of our binaries that are not physical pairs for different separation limits. From this we have chosen an upper separation limit of 1''.5, which implies an 11% contamination, as described below.

### 3.3. Incompleteness

We have tested our completeness of companions by blindly “observing” real stars with artificially added companions (scaled from real stars in the images) at random separations, position angles, and flux ratios. We find that our detections are essentially complete down to separations of 0''.1, a result made possible by the very sharp point spread function of the HST/ACS system. Figure 2 shows two panels with plots of  $\Delta m$  vs. separation in arcseconds. The left panel shows the actual observations of the binaries we detected, while the right panel shows our artificial binaries. Filled circles indicate companions we were able to identify, and empty circles indicate those we failed to see. Our detection limit is essentially complete to 0''.1 except for the largest brightness differences, but very few binaries are found with large flux differences (see Sect. 4.5). To be certain that we are complete, we considered binary companions in the more limited separation range from 0''.15 to 1''.5. However, a much more severe problem with completeness is due to the strong and highly structured emission from the surrounding HII region, a problem that is compounded by our use of images taken through an H $\alpha$  filter. In some areas, especially near the Trapezium, our ability to detect faint stars is diminished, an effect that is unquantifiable but should be kept in mind.

Most binaries that have been found prior to this study were identified using infrared techniques. Whereas all binaries we have detected have been checked against lists of previously discovered binaries, we have not made any systematic effort to check if all these earlier binaries are also detectable in the optical. From random checks it appears that many of these infrared-detected binaries are not visible in our optical images.

### 3.4. Membership of the ONC

The main source for membership information in the ONC are astrometric studies, principally the study by Jones & Walker (1988), which covers the inner  $20' \times 30'$  of the ONC and thus includes our area of study. It is based on photographic I-band plates, which favors red and reddened stars. Of the 1051 stars in our images, 655 stars are listed in the Jones & Walker catalog, and of these 596 have membership probabilities higher than 93%. The large majority of our binaries are not resolved in the JW survey, and thus the proper motions can be affected by relative brightness variations of the components that can shift the photocenter. We have seen such variability in a binary lying in the overlap region between two fields, and thus observed twice. We have also found stars with clear pre-main sequence characteristics that have membership probability of 0%, indicating that astrometric information can be used to *support* membership, but should not be used to *exclude* membership. We are therefore complementing the proper motion membership analysis with other sources, such as X-ray emission,  $H\alpha$  emission, and variability. Getman et al. (2005) has determined that 1373 stars from the 1616 sources in the COUP survey, which largely overlaps with our field (see Figure 1), are Orion members. Among our stars, we find 658 which are detected by COUP and also are classified as ONC members. Finally, we use the presence of  $H\alpha$  emission (partly from the literature and from our own unpublished deep survey), as well as irregular variability as listed in the General Catalogue of Variable Stars. A total of 99 stars were found to have  $H\alpha$  emission. Note that we do not use near-infrared excess as a membership criterion, since our binaries by default are likely to have infrared excesses due to their mostly lower-mass companions. In total, we find 781 stars that have at least one (and commonly several) of

these membership characteristics.

### 3.5. Binaries and Line-of-Sight Pairs

Among the 781 known ONC members detected in our HST images, we found 72 binaries and 3 triples in the range from  $0''.15$  to  $1''.5$ . These are listed in Table 1, where each triple is listed as two binaries, in the manner of counting of Kuiper (1942). The first and second columns list the Jones & Walker ID and the probability of the star to be a member of the ONC based on its proper motion, respectively. The third column lists the Parenago number, the fourth column lists the name in the General Catalog of Variable Stars, the fifth column lists the COUP number, and the sixth column lists the number given by Hillenbrand (1997). The right ascension and declination for equinox 2000 are listed in the seventh and eighth columns. The ninth column lists the position angle of the system and the tenth column lists its separation in arcsec. The apparent magnitude in the I band (from Hillenbrand 1997) is listed in the eleventh column and the difference in magnitudes, in the  $H\alpha$  filter, between the primary and secondary is listed in the twelfth column. The position angle towards and separation (in arcsec) to  $\theta^1$  Ori C are listed in columns 13 and 14, respectively. Then follows the spectral type as listed by SIMBAD. The sixteenth column lists the character of membership for each binary (P: proper motion; X: COUP ONC source; H:  $H\alpha$  emission; V: irregular variable). The last column lists the discovery paper if a binary was known prior to this work.

Additionally, we have found 3 binaries among the ONC members outside the  $60''$  exclusion zone with separations between  $0''.11$  and  $0''.15$ . They are listed in Table 2. We have furthermore examined the optically visible ONC members within the exclusion zone, and have found another 3 binaries with separations less than  $0''.4$ , an (arbitrarily chosen) upper limit we imposed due to the high stellar density in that region. Two of these are new discoveries. Many more binaries have been found by earlier studies of the central region (e.g., Prosser et al. 1994, Padgett et al. 1997, Petr et al. 1998, Simon et al. 1999, Köhler et al. 2006), but most are only detectable in the infrared, since most cluster members are hidden by extinction; these three binaries are the only we could detect in our images in the range  $0''.1 - 0''.4$ . We do not

include the abovementioned binaries in our statistical analysis, but list them in Table 2. Finally, we have searched the 270 stars outside the exclusion zone for which we have no evidence for membership, and have found another 7 binaries. Some of these may be foreground or background stars, but others may turn out to be young stars, and we also list them in Table 2. The columns in Table 2 are the same as in Table 1, except we have added an additional column, which characterizes the binaries.

All of our binaries with known spectral types are late-type stars, presumably classical and weak-line T Tauri stars, with the exception of Parnago 2149 (JW 945), which appears to be a Herbig Ae/Be star.

In Figure 3a,b we show figures of the 78 multiple systems we have identified among ONC members outside the exclusion zone, as well as the three close binaries ( $<0''.4$ ) found inside the exclusion zone. Each stamp is  $2''$  on a side. Some of the binaries are particularly interesting for a variety of reasons, e.g. V1118 Ori is a famous EXor, other binaries or companions are likely substellar objects, and some are associated with jets or proplyds. In the Appendix, we provide more details about these cases.

Could some of the wider binaries in the ONC be due to contamination by line-of-sight pairs? The surface density of stars in the ONC is a steeply declining function of distance from the center of the cluster, with only relatively minor fluctuations due to subclustering (either real or caused by extinction variations, Figure 4). We have determined the stellar density  $\Sigma$  in an area with radius  $30''$  around each of the 781 ONC members, and have determined the probability  $P$  of finding an unrelated star within a distance  $\theta$  from each primary using the expression  $P = 1 - e^{-\pi\theta^2\Sigma}$  (Correia et al. 2006), where we have set  $\theta$  to  $1''.5$ . The probability  $P$  is principally a function of the distance from  $\theta^1$  Ori C, with smaller variations due to local inhomogeneities in the cluster density. Figure 5 shows the distribution of probability of a line-of-sight association for each of the 781 ONC members as a function of distance from  $\theta^1$  Ori C. The figure mostly follows the radial stellar density curve in Figure 4, although the effect of local small-scale groupings is visible.

The sum of contamination probabilities for the

781 stars is 911%. In other words, among the binaries detected we are likely to have roughly 9 line-of-sight doubles. In the following we correct for these false binaries.

## 4. RESULTS

### 4.1. Binary Fraction in ONC

The detection of 72 binaries and 3 triples with separations in the range  $0''.15 - 1''.5$  among the 781 ONC members must be corrected for the estimated 9 binaries that are likely to be due to line-of-sight pairing. Counting the three triples as six binaries, we then have 69 physical binaries, which implies a  $8.8\% \pm 1.1\%$  binary fraction  $bf$  in the interval from 67.5 to 675 AU, or a multiplicity frequency (where the 3 triples are counted as 1 system each) of  $8.5\% \pm 1.1\%$  (here and in the following the error estimates are  $1\sigma$  and are derived using Poisson statistics). Petr et al. (1998) found 4 binaries in the separation range  $0''.14$  to  $0''.5$  in the inner  $40'' \times 40''$  of the Trapezium, corresponding to  $5.9\% \pm 4.0\%$ . In the same limited range of separations we find 50 binaries, corresponding to  $6.4\% \pm 0.9\%$ . The numbers are consistent within their errors.

Reipurth & Zinnecker (1993) observed nearby T Tauri associations and found 38 binaries (of a sample of 238 stars) in the range 150-1800 AU. The range we study statistically is 67.5-675 AU. We have derived the number of binaries in the *common* range 150-675 AU, and find  $11.8\% \pm 2.2\%$  for the associations and  $5.3\% \pm 0.8\%$  in the ONC (for simplicity we here count a triple as two binaries). Both surveys represent *observed* binary fractions, but the Reipurth & Zinnecker survey has negligible incompleteness correction in the chosen range. For our present survey, we have 9 line-of-sight pairs among our 78 binaries, and when we analyze their statistical distribution for different separations, we find that all 9 are likely to be found in the range  $0''.33$  to  $1''.5$ . Of the 50 binaries in the range 150-675 AU we thus should count only 41 as physical binaries, leading to the abovementioned binary percentage of 5.3%. We thus find that the binary fraction in associations is higher by a factor of 2.2 compared to the ONC, in qualitative agreement with the study of Petr et al. (1998), who found a difference of almost a factor of 3 based on small-number statistics.

## 4.2. Separation Distribution Function

In Figure 6 we show the separation distribution of binaries towards the ONC on an angular scale and in bins  $0''.1$  wide. The first bin from  $0''.1$  to  $0''.2$  is incomplete. It is striking that there is clear evidence for structure in the separation distribution function, with a sudden decrease in the number of binaries as the separations increase beyond  $0''.5$ , corresponding to 225 AU. At larger separations, the distribution is quite flat. We return to the physical interpretation of this “wall” in subsequent sections. An early precursor to this result may have been seen by Simon (1997), who studied the two-point correlation function in the ONC based on the results of Prosser et al. (1994) and noted a transition from binary companions to the large-scale cluster at projected separations around 400 AU.

We have made the same plot on a logarithmic scale in Figure 7. The data are essentially complete over the whole separation range displayed. We have corrected the distribution for the 9 line-of-sight pairs by calculating the probability of finding another star within a circle with radius corresponding to the separations of each binary, and then adding these probabilities up for each bin. While such a procedure is meaningless for an individual object, it can be used to distribute the 9 false binaries across the 5 bins. Binaries with the largest separations are most likely to be line-of-sight pairs, and the last bin has a large correction of 6 stars, while three of the four remaining bins each is corrected for one star. Error bars are given for each corrected column.

Figure 7 additionally shows the distribution of field stars in the same interval from Duquennoy & Mayor (1991). The dot-dash curve represents the Gaussian that Duquennoy & Mayor fitted to their entire data set, while the two dashed crosses represent their actual data points within our range. It is evident that the Gaussian is a poor fit to these data points in this specific separation interval. The Duquennoy & Mayor data are given as a function of period, and we have converted these to separations by assuming a mean total binary mass of  $1.2 M_{\odot}$ , appropriate for their sample of F7 to G9 binaries. We have also assumed, as is commonly done, that the projected separation represents the semimajor axis, although statistically there is a

small difference (Kuiper 1935, Couteau 1960).

As noted above, we find a binary frequency (after correcting for the 9 line-of-sight pairs and treating the three triples as six binaries) of  $8.8\% \pm 1.1\%$  in the interval from 67.5 AU to 675 AU. If we calculate the binary frequency from the Duquennoy & Mayor data in the same range, we find a binary frequency of 13.7% using a simple trapezoidal approximation to their log-normal curve, and 12.4% using linear interpolation of their data points. It follows that, in the specific range from 67.5 AU to 675 AU, there is approximately 1.5 times more binaries in the field than in the ONC. We discuss this result further below.

## 4.3. Wide vs Close Binaries as Function of Distance from the Trapezium

We have explored whether there is a difference in the number of wide binaries relative to close binaries as we move from the dense inner cluster regions to the outer reaches of the cluster. Such a difference has been searched for but not found in earlier studies (Köhler et al. 2006). In view of the dramatic change in the separation distribution function at  $0''.5$ , we have chosen this separation as a dividing point, such that we consider binaries between  $0''.15$  and  $0''.5$  as ‘close’ and binaries between  $0''.5$  and  $1''.5$  as ‘wide’. Figure 8 shows the cumulative distributions of these close and wide binaries as function of distance from  $\theta^1$  Ori C in the Trapezium. It is evident from the figure that the two sets of binaries do not have the same radial distribution with increasing distance from the cluster core. To explore this further, we show in Figure 9 the ratio of wide to close binaries as a continuous cumulative distribution, with the first point calculated  $30''$  outside the exclusion zone, that is, at a distance of  $90''$  from  $\theta^1$  Ori C. For each distance, the curve gives the ratio for all binaries from the edge of the exclusion zone to that particular distance. In other words, as the curve moves away from the Trapezium it accounts for more and more binaries, until the last points on the curve represent the mean ratio of wide-to-close binaries for the entire ONC. The dashed lines indicate the  $1\sigma$  errors on the numbers. We have furthermore calculated the same ratio for the Duquennoy & Mayor (1991) binaries, and the two dotted lines indicate the values calculated from their Gaussian fit (lower line) and their actual data points (upper

line). These lines thus represent the ratio for field stars.

The curve does not take into account that 9 of the binaries are likely to be line-of-sight associations. Given that the probability of being a line-of-sight pair increases with separation and with proximity to the center of the ONC, it follows that the curve would dip even deeper down in the inner region if we could remove the 9 non-physical pairs.

It is evident that there is a very pronounced and almost monotonic change in the ratio of wide to close binaries as one moves away from the core of the ONC until a distance of about  $460''$ , at which point the ratio becomes flat. It is also clear that the mean ratio of wide to close binaries for the whole ONC is lower than the Duquennoy & Mayor values. We discuss the implications of these findings in Section 5.

#### 4.4. Higher-order Multiples

In addition to the 72 binaries in the separation range from  $0''.15$  to  $1''.5$ , we have found 3 triple systems with separations in the same range. Tokovinin (2001) suggests that the ratio of triples to binaries is  $0.11 \pm 0.04$  in general, whereas after subtracting the 9 line-of-sight pairs we find  $0.048 \pm 0.01$  in the ONC. Within the considerable errors the numbers are close to being consistent, but it should also be recalled that our survey is restricted to the limited range between the  $0''.15$  completeness limit and the  $1''.5$  confusion limit. It is entirely possible that some close pairs in triple systems have already evolved to become spectroscopic binaries and have thus become unobservable with our detection method. Nor can it be excluded that some wide pairs exist in triple systems with separations larger than  $1''.5$ , although such wide systems cannot be common (Scally et al. 1999). Much better statistics is required to settle the question whether the ONC might be deficient in triple systems.

#### 4.5. Flux Ratios and the Nature of Companions

We have determined the flux-ratios of those of our binaries that are not saturated in our images. Figure 10 shows the resulting histogram as a function of  $\Delta\text{mag}$ . As is well established from other binary studies, the majority of binaries in the ONC

also have unequal components, although the bin with equal components ( $\Delta m < 0.5$  mag.) is the most populated. Only very few of the companions have a magnitude difference to their primary of more than 2.5 magnitudes.

In the absence of spectroscopic information, we have made a crude attempt to investigate the nature of the companions based on their measured flux ratios. In order to do that we have made some assumptions. First, we assume that the observed flux ratios reflect the photospheric fluxes, in other words that  $H\alpha$  emission line fluxes are not seriously affecting the ratios. This may not always be a good assumption, since mid-to-late M dwarfs often are very active, and their photospheric fluxes are so low that  $H\alpha$  line emission could be a significant contribution. If we mistake  $H\alpha$  line emission for photospheric flux from the primary, our estimate of a spectral type for a companion will be earlier than it is in reality. Second, most published photometry of late-type dwarfs is broad-band, whereas we have observed in the narrow-band  $H\alpha$  filter, so we assume that our observed magnitude differences can be compared to R-band photometry. Since we are dealing with the difference between two stars, this is probably not a bad assumption, at least when the flux ratio is not large. Third, we assume that the observed flux ratios are not affected by differences in extinction between the components. Given the young age and occasional association with molecular clouds, this may not in all cases hold true.

With these caveats spelled out, we have used the  $M_I$  vs spectral type relation and the R-I colors for M dwarfs (e.g., Dahn et al. 2002) to derive the difference in R-band magnitudes as a function of spectral type for M-dwarfs. The relation turns out to be essentially linear, with a mean drop of 0.56 magnitudes per spectral subtype throughout the M spectral range. We then used the spectral classifications for the primaries provided by SIMBAD, of mixed provenance, with our flux ratios to estimate a spectral type for the secondaries. For a cluster with an age between 0.5 and 3 Myr, the substellar limit is around spectral type M6.25 following the models of Baraffe et al. (1998) and Chabrier et al. (2000) and using the temperature scale of Luhman et al. (2003), see also Luhman et al. (2006). To our surprise, quite a number of the secondaries appear to be brown dwarfs, in

at least one case forming a wide BD-BD binary. We comment on selected cases in the Appendix. Given the assumptions involved and the simplistic nature of these spectral type estimates, it is obvious that spectroscopy is required to establish the true nature of the secondaries.

## 5. DISCUSSION

### 5.1. Structure and Evolution of the Separation Distribution Function

The separation distribution function of field binaries has been approximated by various functions. Öpik (1924) suggested that binaries with separations larger than  $\sim 60$  AU follow a  $f(a) \sim 1/a$  distribution, whereas Kuiper (1942) proposed that the overall distribution could be represented by a Gaussian. The latter distribution was adopted as a good fit to their data in the influential study by Duquennoy & Mayor (1991), although it is evident from Figure 7 that in the specific separation range discussed in the present paper, the Gaussian is a poor approximation to the actual data. Integrating the Öpik relation over logarithmic bins results in a straight horizontal line to describe the logarithmic separation distribution, and this is clearly a better fit to the two data points of Duquennoy & Mayor seen in Figure 7. The Öpik relation has also been supported by numerous studies summarized by Poveda & Allen (2004).

For the separation distribution of ONC binaries (corrected for line-of-sight associations) both a Gaussian and a horizontal line provide acceptable fits to the data when considering the uncertainties of the data points. It is thus not possible to classify the structure of the ONC separation distribution function with the available data.

The separation distribution function in the ONC most probably has not yet found its final shape. Two basic mechanisms operate that can affect the orbit of a young binary: rapid dynamical decay in small-N clusters (e.g., Sterzik & Durisen 1998, Reipurth & Clarke 2001, Bate et al. 2002) and the passage of a binary through a dense cluster (e.g., Kroupa 1995a,b, Kroupa et al. 1999). The former occurs primarily during the Class 0 phase (Reipurth 2000), and is no longer relevant for stars in the ONC. The latter, however, may be essential for understanding the binary population of the ONC. A wide binary falling through

the potential well of a cluster will gain kinetic energy through encounters, and binaries with weak binding energies are eventually disrupted (Heggie 1975). A prediction of this scenario is that binaries at distances from the cluster center larger than the corresponding crossing time should not be showing any dynamical alterations due to encounters with other cluster members (Kroupa et al. 1999, 2001). The crossing time of a star through a cluster is  $t_{cross} = 2R/\sigma$ , where  $R$  is the cluster radius and  $\sigma$  is the mean one-dimensional velocity dispersion in the cluster. Assuming that this velocity dispersion in the ONC is of the order of  $2 \text{ km s}^{-1}$  (e.g., Jones & Walker 1988), we have in Figure 9 indicated the crossing time for different distances to the cluster center. The figure suggests that for distances larger than roughly 460 arcsec there is no longer a measurable change in the ratio of wide-to-close binaries. Given that the wide-to-close binary ratio changes by a factor of 4-5 from the inner to the outer regions, this suggests that many, and perhaps most, of the wide binaries are disrupted after only a few passages of the cluster center. The variation of the ratio of wide-to-close binaries from the inner to the outer regions of the ONC, seen in Figure 9, offers the first compelling observational evidence that dynamical interactions in the dense central region of the ONC have taken place.

In principle, the diagram in Figure 9 allows us to determine the age of the ONC. An angular distance of  $\sim 460$  arcsec corresponds to a crossing time of about 1 million years. However, an age determined in this manner is directly dependent on the velocity dispersion assumed. Therefore, all we can say about the age of 1 million years we estimate for the ONC is that it is consistent with other ONC age estimates (e.g., Hillenbrand 1997).

The significantly lower number of binaries that we find in the ONC compared to associations thus appears to be due, at least in part, dissolution of wide binaries. However, under certain circumstances an encounter could lead to hardening of the binary, making it closer than our resolution limit, so it is not lost to the overall binary budget.

Even in its outermost regions, the ONC shows a smaller ratio of wide-to-close binaries than seen in the field by Duquennoy & Mayor (1991). Considering that the majority of field stars are likely to have been formed in a cluster, it follows that

many of the *wide* binaries in the field must have formed in the gentler environment of a loose T association.

Durisen & Sterzik (1994) found, on theoretical grounds, that binaries are more likely to form in clouds with lower temperatures. Reipurth & Zinnecker (1993) found observational evidence that clouds with more stars have relatively fewer binaries in the separation range under study (mostly wide visual binaries). Both these results could indicate that loose T associations produce or retain more wide binaries than do clusters. However, Brandeker et al. (2006) noted that the young sparse  $\eta$  Chamaeleontis cluster has a deficit of wide binaries. Unless this small cluster is the remnant of a much denser cluster, then this result would seem to be in contradiction to the notion that wide binaries are preferentially formed/preserved in loose associations.

In any case, there is no question that the field binary population is a mix of binaries formed in clusters and in associations. We can attempt to calculate the fraction of stars that originate in clusters and in associations. In Sect. 4.2 we showed that, in the limited separation range 67.5 - 675 AU, the binary fraction of the field stars of Duquennoy & Mayor (1991) is about a factor 1.5 higher than in the ONC. We also found that in the range 150 - 675 AU associations have a factor 2.2 more binaries than the ONC. In other words, in these limited ranges associations have about 1.5 times as many binaries as the field population, and the ONC has only about 2/3 as many binaries as the field population. It follows that the field star binary population in principle can be produced if only 1/3 of binaries come from the binary-rich associations and 2/3 originate in binary-poor ONC-type clusters, in excellent agreement with the results of Patience et al. (2002) and in approximate agreement with findings that 70-90% of all stars may be formed in clusters (e.g., Lada & Lada 2003). Of course, this assumes that the binary ratios between field stars, associations, and the ONC derived here within narrow separation ranges can be extrapolated to all separations, an assumption that may not hold at all.

## 5.2. Very Low Mass Stellar and Substellar Companions

As noted in Sect. 4.5, spectroscopy is required to determine the true nature of the companions we have found. However, unless significant extinction differences are common among our binaries, then the difference in component brightness, combined with spectral type estimates for the primaries when available, are indicative of the spectral types of the secondaries. While this is highly uncertain in individual cases, overall it is likely to be indicative of the properties of the companion population. Table 1 lists the spectral types for 46 primaries, and of these 38, or 83%, are M-type stars. We find that more than half (25) of these 46 binary stars have secondaries with spectral types of M5 or later, and about one third (17) could be substellar. These numbers are upper limits, since we cannot correct for the 9 false binaries that we expect to be present in our sample of 78 multiple systems, but they are probably more likely to be found among pairs with faint, widely separated companions. However, even if we subtracted all 9 objects from the 17 that could be substellar, this would still indicate that 8, or about 17%, of the 46 binaries with spectral type estimates are likely to have substellar companions. Selected cases are discussed in the Appendix.

The closest binaries we were able to resolve with our imaging technique have projected separations of 50 AU. All of the binaries with likely substellar companions are thus quite wide, which is of interest for formation theories (see, e.g., Lucas et al. 2005, and reviews by Burgasser et al. 2007, Luhman et al. 2007, Whitworth et al. 2007).

It is likely that there are several brown dwarf – brown dwarf binaries in our binary sample, but the only one that we are certain of is COUP 1061. Infrared spectroscopy of this source indicates a spectral type of M9-L0 (Meeus & McCaughrean 2005). We have resolved this object into two components with almost equal brightness and a projected separation of 100 AU. Brown dwarf binaries with such large separations are rare (e.g., Lucas et al. 2005, Allen et al. 2007), although a few very wide pairs are known (e.g., Artigau et al. 2007, Barrado y Navascués et al. 2007).



## 6. CONCLUSIONS

We have analyzed a large set of  $H\alpha$  images of the Orion Nebula Cluster acquired with the Hubble Space Telescope and the Advanced Camera for Surveys with the goal of detecting binaries among a sample of 781 ONC members. The following results were obtained:

1. A total of 75 binaries and 3 triple systems were detected, of which 55 are new discoveries.

2. Within the limited angular range of  $0''.15$  to  $1''.5$ , corresponding to projected separations of 67.5 AU to 675 AU, we have found a binary fraction of  $8.8\% \pm 1.1\%$  after correcting for a statistically determined contamination of 9 line-of-sight binaries.

3. The field binary fraction for solar type stars in the same separation range is 1.5 times larger, and for T Tauri associations it is 2.2 times larger than in the ONC, confirming earlier results that the ONC is deficient in binaries, now with statistically significant data.

4. The separation distribution function for young binaries in the ONC shows a dramatic decrease in binaries for angular separations larger than  $0.5''$ , corresponding to projected separations of 225 AU.

5. The ratio of cumulative distributions of wide ( $0''.5$  to  $1''.5$ ) to close ( $0''.15$  to  $0''.5$ ) binaries show an increase out to a distance of about  $460''$  from the center of the ONC, after which it levels out. We interpret this as clear observational evidence for dynamical evolution of the binary population as a result of passages through the potential well of the ONC. These results are consistent with an age of the ONC of about 1 million yr.

6. It appears that much of the deficiency of binaries in the ONC compared to the field star population can be understood, at least in part, in terms of the destruction of wide binaries combined with a secondary effect from orbital evolution of binaries towards closer separations that are unobservable in direct imaging surveys.

7. Limited spectral information about the primary stars indicate that they are low mass T Tauri stars (except for one Herbig Ae/Be star). Assuming that most binaries are not affected by differential extinction, we find that possibly as many as 50% of the binaries have companions with spec-

tral types later than M5, and from 1/6 to 1/3 of the binaries may have substellar companions, all of which with separations of at least 50 AU. This large number of wide substellar companions is of interest for theories of brown dwarf formation.

We thank Rainer Köhler, Pavel Kroupa, Luiz Paulo Vaz, and Adam Burgasser for valuable comments, and an anonymous referee for a very helpful referee report. We are grateful to Burton Jones for providing us an electronic version of the Jones & Walker (1988) proper motion table. Marcelo Guimarães acknowledges financial support by CAPES, CNPq and FAPEMIG. Based on observations taken under program GO-9825 with the NASA/ESA Hubble Space Telescope obtained at the Space Telescope Science Institute, which is operated by the Association of Universities for Research in Astronomy, Inc., under NASA contract NAS5-26555. This material is based upon work supported by the National Aeronautics and Space Administration through the NASA Astrobiology Institute under Cooperative Agreement No. NNA04CC08A issued through the Office of Space Science. This research has made use of the SIMBAD database, operated at CDS, Strasbourg, France, and NASA's Astrophysics Data System Bibliographic Services.

## A. Appendix. Individual Binaries of Interest.

In the following, comments are provided on binaries of particular interest, especially regarding possible substellar companions.

**V1438 Ori** (JW 39). The spectral type of M3 is due to Hillenbrand (1997). If the 2.6 mag brightness difference is not affected by extinction differences, then the companion is an M8 brown dwarf at a projected separation of 170 AU. Stassun et al. (1999) detected lithium in the primary.

**JW 71.** The spectral type of M4 is due to Hillenbrand (1997). If the 1.4 mag brightness difference is not affected by extinction differences, then the companion is an M7 brown dwarf with a projected separation of 90 AU.

**V1118 Ori** (JW 73). This is a member of the class of EXor's (Herbig 1989). The star, which is also known as Chanal's Object, has had 5 outbursts since its discovery in 1984, and typically varies within the range  $14.5 < V < 18$ , with a rise time of less than a year and a declining phase about twice as long. Optical and infrared spectroscopy of V1118 Ori is reported by Parsamian et al. (2002) and Lorenzetti et al. (2006), and X-ray observations are analyzed by Audard et al. (2005). The discovery that V1118 Ori has a companion only 0.4 magnitude fainter in the H $\alpha$  filter raises interesting questions about which of the components that may drive the variability (Herbig 2007).

**JW 121.** The spectral type of M3 is due to Hillenbrand (1997). If the 3.0 mag brightness difference is not affected by extinction differences, then the companion is an M8 brown dwarf with a projected separation of 153 AU.

**JW 147.** The spectral type of M5 is due to Hillenbrand (1997). If the 1.4 mag brightness difference is not affected by extinction differences, then the companion is an M8 brown dwarf with a projected separation of 135 AU.

**JW 152.** The spectral type of M3 is due to Hillenbrand (1997). If the 2.5 mag brightness difference is not affected by extinction differences, then the companion is an M7 brown dwarf with a projected separation of 81 AU.

**JW 235.** JW 235 is associated with the HH 504 object, discovered by Bally & Reipurth (2001), see also O'Dell (2001). The binarity of the star was discovered by Köhler et al. (2006). Its proper motion in the Jones & Walker catalog implies that it has 0% probability of being a member of the ONC. However, given the similar brightness of the two components, it is likely that brightness variations of the stars shifted the photocenter used for astrometry. Evidence for ONC membership is strong and is based on the presence of H $\alpha$  emission, detection in X-rays, optical variability, and association with an HH object.

**V1274 Ori** (JW 248). The spectral type of the primary is somewhat in dispute. Hillenbrand (1997) suggests M0.5-M2 (with the Ca II lines in emission), Edwards et al. (1993) suggest M3, and Meeus & McCaughrean (2005) suggest M0-M4. The binarity of the system was found by the COUP survey. Our primary is the secondary in the COUP catalog, indicating that our secondary is highly X-ray active. Sicilia-Aguilar et al. (2005) detected lithium in the (optical) primary, and found an inverse P Cygni profile at H $\alpha$ . If there is not an extinction difference between the primary and secondary, then the large flux difference ( $>3.7$  mag) suggests that the companion could be an L0 brown dwarf. However, the system is only 3 arcmin from  $\theta^1$  Ori C, so there is a 1% chance of a line-of-sight association.

**JW 296.** JW 296 is the primary of a hierarchical triple system. The secondary and tertiary are very faint stars, surrounded by a common proplyd-like envelope known as 066-652 (O'Dell & Wong 1996). The primary is of spectral type M4.5 according to Hillenbrand (1997). If the brightness difference is taken at face value, the secondary and tertiary should be L0 brown dwarfs, but given the obvious association with nebulosity it is likely that their faintness is merely due to extinction.

**JW 355.** The primary of this system is located at the edge of a proplyd known as 109-246 (O'Dell & Wong 1996). The proper motion of the star suggests it is not an ONC member, but it is found to be a member by the COUP project. Hillenbrand (1997) suggests a mid-K spectral type. The system is only 90'' from  $\theta^1$  Ori C, and the star density is so high that the possibility of a line-of-sight association is several

percent.

**JW 370.** There is a silhouette disk close ( $\sim 3''/4$ ) to this binary. Given the local density of stars around this system, the probability that such a silhouette disk is just a chance alignment is  $\sim 7\%$ . The chance of a line-of-sight alignment for the binary itself is 1.5%. Hillenbrand (1997) suggests a spectral type of K0-K3.

**V1492 Ori (JW 383).** The primary is of spectral type M3 according to Hillenbrand (1997). If the 2.1 mag brightness difference is not affected by extinction differences, then the companion is an M7 brown dwarf with a projected separation of 86 AU. Stassun et al. (1999) derive a rotation period of 7.11 days for the primary, and notes the presence of lithium in the spectrum.

**Paranago 1806 (JW 391).** The primary is of spectral type M1 according to Edwards et al. (1993) and Hillenbrand (1997), who also notes the presence of Ca II emission. The primary is saturated in our images, but with a magnitude difference of at least 3.3 mag, the companion would be an M7 brown dwarf if there is no difference in extinction. However, the pair is located in a region of high stellar density, so the probability of a chance alignment is more than 5%.

**JW 509.** This binary was first detected by Prosser et al. (1994) and subsequently by Padgett et al. (1997) and Lucas et al. (2005). Although it is a well known binary it does not have a spectral type in the literature. Since this system is located in a crowded region, the probability of a chance alignment is  $\sim 2.7\%$ , but the reality of the binary is supported by an interaction zone between the stars, visible in our image (Fig. 3b).

**Paranago 1914 (JW 551).** The primary of this hierarchical triple system has a spectral type M1 according to Hillenbrand (1997). The tertiary is not detectable either in the optical or in X-rays, and since its separation from the primary is as large as  $1''/27$  it could be a background object. The system seems to be part of a small subcluster, which gives it a high probability of a chance alignment ( $\sim 2.2\%$ ). Given the primary spectral type, the difference in magnitudes to the tertiary (3.6) and assuming that the tertiary is not a background object, the tertiary could have a spectral type M7 or M8 and thus would be a brown dwarf candidate.

**COUP 967.** This star was catalogued as a binary by Prosser et al. (1994), Padgett et al. (1997) and Lucas et al. (2005). Our image shows that the primary is associated with a proplyd (184-427 in O'Dell & Wong 1996) and the secondary is a faint object ( $\Delta m_{H\alpha} = 2.4$ ). The spectral type for the primary is M2.5 according to Hillenbrand (1997). The system is very close to  $\theta^1$  Ori C ( $\sim 70''$ ) and the probability of a chance alignment is 3.5%. If the components have the same extinction, then the secondary would be of spectral type M6.5, and thus at the hydrogen burning limit.

**JW 592.** The spectral type M2.5 is due to Hillenbrand (1997) and M4 according to Edwards et al. (1993). The brightness difference (4 magnitudes) would imply an M9.5 spectral type or later for the secondary, making it a brown dwarf with a projected separation of  $\sim 275$  AU.

**COUP 1061.** This very close system ( $\sim 100$  AU) has a combined spectral type M9-L0 according to Meeus & McCaughrean (2005), who did not resolve it, and since the components have virtually the same brightness, this is therefore a *bona fide* brown dwarf - brown dwarf binary with a projected separation of 100 AU.

**V1524 Ori (JW 681).** This binary was first catalogued by Prosser et al. (1994) and has a spectral type K7 according to Prosser & Stauffer (unpublished). The secondary is associated with the proplyd 213-346 (O'Dell & Wong 1996). In the Hillenbrand (1997) catalog this system has two entries, both with number 681 but with different coordinates. SIMBAD identifies three different objects: H97b-681, H97b-681a, and H97b-681b. The first is JW 681, also known as V1524 Ori, and is the primary in this double. The second is the unrelated object MLLA 312, and the third is the X-ray source COUP 1149, which forms the secondary component, associated with the proplyd. Because this system is located near to  $\theta^1$  Ori C ( $\sim 77''$ ) the probability of a chance alignment is 3.5%.

**V1528 Ori (JW 727).** The spectral type M2 is due to Hillenbrand (1997) and the difference in brightness suggests a spectral type of L0 for the companion if the components have the same extinction. If so, the secondary is a brown dwarf with projected separation of 329 AU. The primary shows H $\alpha$  emission according

to our unpublished survey.

**JW 748.** This binary was discovered by Prosser et al. (1994), and the spectral type of the primary is M3 according to Hillenbrand (1997). Given the brightness difference and if the components have the same extinction, the secondary could be a brown dwarf with spectral type M7 and a projected separation of 158 AU.

**JW 767.** First discovered by Köhler et al. (2006) this system has a spectral type M2.5 due to Hillenbrand (1997). The secondary has a silhouette disk and is associated with the HH 668 object (Bally et al. 2006). The extinction caused by the silhouette disk probably is responsible for the large difference in brightness by more than 4 magnitudes between the primary and secondary.

**Paréngo 2075** (JW 867). This object was observed by Köhler et al. (2006) but despite its brightness and separation ( $0''.29$ ) they did not resolve it, suggesting possible major variability of the secondary. The system presents evidence of H $\alpha$  emission, X-rays and optical variability. A spectral type of M1 was suggested by Blanco (1963), and more recently Duncan (1993) assigned a spectral type of K8Ve. Sicilia-Aguilar et al. (2005) reported lithium in the spectrum of the primary.

**JW 906.** The primary is of spectral type M3 according to Hillenbrand (1997), and if the difference in brightness (2.7 mag) is not affected by extinction then the secondary is a brown dwarf with spectral type M8 and a large projected separation of 625 AU. Sicilia-Aguilar et al. (2005) reported lithium in the spectrum of the primary.

## REFERENCES

- Allen, P.R., Koerner, D.W., McElwain, M.W., Cruz, K.L., & Reid, I.N. 2007, *AJ*, 133, 971
- Artigau, E., Lafrenière, D., Doyon, R., Albert, L., Nadeau, D., & Robert, J. 2007, *ApJ*, 659, L49
- Audard, M., Güdel, M., Skinner, S.L., Briggs, K.R., Walter, F.M. et al. 2005, *ApJ*, 635, L81
- Bally, J. & Reipurth, B. 2001, *ApJ*, 546, 299
- Bally, J., Licht, D., Smith, N., & Walawender, J. 2006, *AJ*, 131, 473
- Baraffe, I., Chabrier, G., Allard, F., & Hauschildt, P.H. 1998, *A&A*, 337, 403
- Barrado y Navascués, D., Bayo, A., Morales-Calderón, M., Huélamo, N., Stauffer, J.R., & Bouy, H. 2007, *å*, in press
- Bate, M.R., Bonnell, I.A., & Bromm, V. 2002, *MNRAS*, 336, 705
- Blanco, V.M. 1963, *ApJ*, 137, 513
- Brandeker, A., Jayawardhana, R., Khavari, P., Haisch, K.E., & Mardones, D. 2006, *ApJ*, 652, 1572
- Burgasser, A.J., Reid, I.N., Siegler, N., Close, L., Allen, P., Lowrance, P., & Gizis, J. 2007, in *Protostars and Planets V*, eds. B. Reipurth, D. Jewitt, & K. Keil, Univ. of Arizona Press, 427
- Chabrier, G., Baraffe, I., Allard, F., & Hauschildt, P.H. 2000, *ApJ*, 542, 464
- Choi, P.I. & Herbst, W. 1996, *AJ*, 111, 283
- Correia, S., Zinnecker, H., Ratzka, Th., & Sterzik, M.F. 2006, *A&A*, 459, 909
- Couteau, P. 1960, *Journ. des Observateurs*, 43, 41
- Dahn, C.C., Harris, H.C., Vrba, F.J., Guetter, H.H., Canzian, B., Henden, A.A. et al. 2002, *AJ*, 124, 1170
- Duchêne, G. 1999, *A&A*, 341, 547
- Duchêne, G., Bouvier, J., Bontemps, S., André, P., & Motte, F. 2004, *A&A*, 427, 651
- Duncan, D.K. 1993, *ApJ*, 406, 172
- Duquennoy, A. & Mayor, M. 1991, *A&A*, 248, 485
- Durisen, R.H. & Sterzik, M.F. 1994, *A&A*, 286, 84
- Edwards, S., Strom, S.E., Hartigan, P., Strom, K.M., Hillenbrand, L.A. et al. 1993, *AJ*, 106, 372
- Getman, K.V., Feigelson, E.D., Grosso, N., McCaughrean, M.J., Micela, G. et al. 2005, *ApJS*, 160, 353
- Heggie, D.C. 1975, *MNRAS*, 173, 729
- Herbig, G.H. 1962, *Adv. Astr. Astrophys.*, 1, 47
- Herbig, G.H. 1982, in *Symp. on the Orion Nebula to Honor Henry Draper*, ed. A.E. Glassgold & P.J. Huggins, New York Acad. Sci., 64
- Herbig, G.H. 1989, in *ESO Workshop on Low Mass Star Formation and Pre-Main Sequence Objects*, ed. Bo Reipurth, p.233
- Herbig, G.H. 2007, in prep.
- Herbig, G.H. & Terndrup, D.M. 1986, *ApJ*, 307, 609
- Hillenbrand, L.A. 1997, *AJ*, 113, 1733
- Jones, B.F. & Walker, M.F. 1988, *AJ*, 95, 1755
- Joy, A.H. & van Biesbroeck, G. 1944, *PASP*, 56, 123
- Kroupa, P. 1995a, *MNRAS*, 277, 1491
- Kroupa, P. 1995b, *MNRAS*, 277, 1507
- Kroupa, P. 2000, *New Astronomy*, 4, 615
- Kroupa, P., Petr, M.G., & McCaughrean, M.J. 1999, *New Astronomy*, 4, 495
- Kroupa, P., Aarseth, S., & Hurley, J. 2001, *MNRAS*, 321, 699
- Kuiper, G.P. 1935, *PASP*, 47, 121
- Kuiper, G.P. 1942, *ApJ*, 95, 201
- Köhler, R., Petr-Gotzens, M. G., McCaughrean, M. J., Bouvier, J., Duchêne, G. et al. 2006, *A&A*, 458, 461
- Lada, C.J. & Lada, E.A. 2003, *Ann. Rev. Astron. Astrophys.* 41, 57

- Lorenzetti, D., Giannini, T., Calzoletti, L., Pucetti, S., Antonucci, S. et al. 2006, *A&A*, 453, 579
- Lucas, P.W., Roche, P.F., & Tamura, M. 2005, *MNRAS*, 361, 211
- Luhman, K.L., Stauffer, J.R., Muench, A.A., Rieke, G.H., Lada, E.A., Bouvier, J., & Lada, C.J. 2003, *ApJ*, 593, 1093
- Luhman, K.L., Whitney, B.A., Meade, M.R., Babler, B.L., Indebetouw, R., Bracker, S., & Churchwell, E.B. 2006, *ApJ*, 647, 1180
- Luhman, K.L., Joergens, V., Lada, C., Muzerolle, J., Pascucci, I., & White, R. 2007, in *Protostars and Planets V*, eds. B. Reipurth, D. Jewitt, & K. Keil, Univ. of Arizona Press, 443
- Meeus, G. & McCaughrean, M.J. 2005, *AN*, 326, 977
- O'Dell, C.R. 2001, *AJ*, 122, 2662
- O'Dell, C.R. & Wong, K. 1996, *AJ*, 111, 846
- Padgett, D.L., Strom, S.E., & Ghez, A. 1997, *ApJ*, 477, 705
- Parsamian, E.S., Mujica, R., & Corral, L. 2002, *Astrophysics*, 45, 393
- Patience, J., Ghez, A.M., Reid, I.N., & Matthews, K. 2002, *AJ*, 123, 1570
- Petr, M.G., Coudé du Foresto, V., Beckwith, S., Richichi, A., & McCaughrean, M.J. 1998, *ApJ*, 500, 825
- Poveda, A. & Allen, C. 2004, *Rev. Mex. Astron. Astrofis. Ser. Conf.* 21, 49
- Preibisch, T., Balega, Y., Hofmann, K.-H., Weigelt, G., & Zinnecker, H. 1999, *New Astron.*, 4, 531
- Prosser, C.F., Stauffer, J.R., Hartmann, L., Soderblom, D.R., Jones, B.F. et al. 1994, *ApJ*, 421, 517
- Ratzka, T., Köhler, R., & Leinert, Ch. 2005, *A&A*, 437, 611
- Reipurth, B. 2000, *AJ*, 120, 3177
- Reipurth, B. & Clarke, C.J. 2001, *AJ*, 122, 432
- Reipurth, B. & Zinnecker, H. 1993, *A&A*, 278, 81
- Scally, A., Clarke, C.J., & McCaughrean, M.J. 1999, *MNRAS*, 306, 253
- Sicilia-Aguilar, A., Hartmann, L.W., Szentgyorgyi A.H., Fabricant, D.G., Fürész, G. et al. 2005, *AJ*, 129, 363
- Simon, M. 1997, *ApJ*, 482, L81
- Simon, M., Ghez, A. M., Leinert, Ch., Cassar, L., Chen, W. P. et al. 1995, *ApJ*, 443, 625
- Simon, M., Close, L.M., Beck, T.L. 1999, *AJ*, 117, 1375
- Stassun, K.G., Mathieu, R.D., Mazeh, Tsevi, & Vrba, F.J. 1999, *AJ*, 117, 2941
- Sterzik, M.F. & Durisen, R.H. 1998, *A&A*, 339, 95
- Tokovinin, A. 2001, in *IAU Symp. No.200 The Formation of Binary Stars*, eds. H. Zinnecker & R.D. Mathieu, p.84
- Öpik, E. 1924, *Tartu Obs. Publ.*, 25, No. 6
- Whitworth, A., Bate, M.R., Nordlund, A., Reipurth, B., & Zinnecker, H. 2007, in *Protostars and Planets V*, eds. B. Reipurth, D. Jewitt, & K. Keil, Univ. of Arizona Press, 459

---

This 2-column preprint was prepared with the AAS L<sup>A</sup>T<sub>E</sub>X macros v5.2.

TABLE 1  
 PRE-MAIN SEQUENCE BINARIES WITH ANGULAR SEPARATION BETWEEN 0''15 AND 1''5, OUTSIDE THE 60''  
 EXCLUSION ZONE AROUND  $\theta^1$  ORI C.

JW	%	Par	GCVS	COUP	H97	RA <sub>2000</sub>	DEC <sub>2000</sub>	PA	SEP ["]	$m_I$	$\Delta m_{H\alpha}^1$	PA <sub>OriC</sub>	OriC	SpT <sup>2</sup>	Memb. <sup>3</sup>
39	99	...	V1438	...	39	5:34:38.1	-5:27:41	21	0.38	14.29	2.6	246	628	M3	PV
52	98	...	...	...	52	5:34:40.8	-5:28:09	231	0.20	14.58	0.1	242	604	M5	P
63	99	1569	V1441	17	63	5:34:43.0	-5:20:07	0	0.27	12.75	1.5	291	537	K6	PXV
71	99	...	...	21	71	5:34:44.5	-5:24:38	105	0.20	15.61	1.4	261	483	M4	PX
73	99	...	V1118	...	73	5:34:44.7	-5:33:42	329	0.18	14.04	0.4	217	779	M1	PHV
81	97	1600	...	28	81	5:34:46.4	-5:24:32	272	1.34	12.91	1.9	261	454	M0	PXV
121	99	...	...	...	121	5:34:51.2	-5:16:55	200	0.34	14.90	3.0	316	541	M3	PV
124	99	...	...	64	124	5:34:51.8	-5:21:39	200	0.48	13.94	0.0	286	382	M3.5	PXV
127	99	...	...	66	127	5:34:52.1	-5:24:43	254	0.48	14.28	0.6	258	373	M3.5	PXHV
128	97	...	V1458	67	128	5:34:52.2	-5:22:32	215	0.39	12.64	>0.6	278	366	M2.5	PXHV
135	99	...	V1460	72	135	5:34:52.7	-5:29:46	11	0.40	14.45	0.1	223	522	M3	PXV
147	99	...	...	...	147	5:34:54.4	-5:17:21	26	0.30	14.80	1.4	318	489	M5	P
151	99	...	...	95	151	5:34:54.8	-5:25:13	332	0.15	15.44	1.6	251	341	M3	PX
152	99	...	...	96	152	5:34:55.1	-5:25:30	51	0.18	14.12	2.5	248	343	M3	PX
176	99	1673	KQ	123	176	5:34:57.8	-5:23:53	336	1.28	11.58	>1.1	264	280	K8	PXV
190	99	...	...	134	190	5:34:59.3	-5:23:33	355	0.56	15.33	0.3	268	256	M6	PX
201	99	...	...	150	201	5:35:01.0	-5:24:10	246	1.09	13.41	0.8	258	235	M2.5	PXH
222	98	...	V1320	174	222	5:35:02.2	-5:29:10	89	1.07	14.14	1.4	212	407	M2	PXV
223	99	...	...	177	223a	5:35:02.4	-5:20:47	130	0.34	13.64	1.3	307	261	...	PX
224	99	...	...	180	224	5:35:02.7	-5:19:45	164	0.27	15.38	2.4	317	299	M1	PXV
235	0	...	...	197	235	5:35:03.6	-5:29:27	346	0.54	13.69	0.4	208	411	...	PXHV
248	99	...	V1274	214	248	5:35:04.4	-5:23:14	320	0.90	12.73	>3.7	273	180	M3	PXV
-	-	...	...	260	3064	5:35:06.2	-5:22:13	284	0.40	16.20	0.3	295	169	M4	X
296	99	...	...	275	296	5:35:06.6	-5:26:51	196	0.89	14.30	3.2	215	255	M4.5	PX
296	99	...	...	275	296	5:35:06.6	-5:26:52	158	0.27	14.30	0.4	215	256	M4.5	PX
305	99	...	...	...	305	5:35:07.6	-5:24:01	302	0.45	14.58	0.3	254	137	M3	PV
355	0	...	...	403	355	5:35:10.9	-5:22:46	197	0.42	15.03	3.5	294	90	K:	X
370	99	...	...	452	370	5:35:11.9	-5:19:26	122	0.73	13.86	3.5	344	246	K1.5	PX
383	99	...	V1492	489	383	5:35:12.7	-5:16:14	280	0.19	14.57	2.1	353	433	M3	PXV
392	99	...	...	498	392	5:35:12.7	-5:27:11	185	0.23	15.21	0.2	194	234	M6	PX
391	99	1806	...	501	391	5:35:12.8	-5:20:44	94	0.29	12.97	>3.3	341	168	M1	PXV
399	99	...	...	523	399b	5:35:13.2	-5:22:21	345	0.22	16.77	0.1	322	78	...	PX
410	99	...	...	...	410	5:35:13.2	-5:36:18	167	1.19	16.00	1.3	184	777	...	PV
406	99	...	V1327	543	406	5:35:13.5	-5:17:10	271	0.95	13.88	2.6	353	375	M1	PXV
-	-	...	...	562	9048	5:35:13.6	-5:21:21	62	0.24	16.27	1.5	341	129	M3	X
422	99	...	V1495	566	422	5:35:13.7	-5:28:46	74	0.31	14.43	0.0	187	326	...	PXV
436	0	...	...	620	436a	5:35:14.3	-5:22:04	238	0.32	16.97	1.0	338	85	...	X
439	99	...	V1329	626	439	5:35:14.5	-5:17:25	150	0.30	14.97	0.1	355	359	M1	PXV
439	99	...	V1329	626	439	5:35:14.5	-5:17:25	78	1.21	14.97	4.1	355	359	M1	PXV
444	99	...	...	651	444	5:35:14.6	-5:16:46	190	0.18	15.53	1.0	356	398	...	PX
445	26	...	...	645	445a	5:35:14.7	-5:20:42	191	0.44	14.67	1.8	351	163	...	X
-	-	...	V1500	...	466	5:35:14.9	-5:36:39	82	0.38	14.45	2.2	182	797	...	V
465	97	1875	V409	...	465	5:35:14.9	-5:38:06	271	0.43	14.71	4.1	182	883	...	PV
498	99	1873	V1504	...	498	5:35:15.8	-5:32:59	122	0.70	13.81	0.2	181	576	...	PHV
509	99	...	...	789	509a	5:35:16.2	-5:24:56	46	0.49	15.06	0.1	182	93	...	PXV
511	99	...	...	...	511a	5:35:16.3	-5:22:10	241	0.41	15.67	2.4	358	73	M1	PX
-	-	...	...	822	3031	5:35:16.8	-5:17:17	84	0.26	16.37	0.5	1	366	...	X
551	99	1914	...	881	551a	5:35:17.4	-5:25:45	265	0.14	13.87	0.0	174	142	M1	PX
551	99	1914	...	881	551a	5:35:17.4	-5:25:45	262	1.27	13.87	3.6	174	143	M1	PX
552	99	1908	V410	897	552a	5:35:17.5	-5:21:46	156	0.46	14.50	>1.8	9	99	...	PXV
560	98	...	V1334	927	560	5:35:17.9	-5:15:33	235	0.60	14.17	3.2	3	471	...	PXV
570	99	...	...	937	570a	5:35:17.9	-5:25:34	0	0.15	14.73	0.8	170	133	...	PX
566	0	...	...	939	566	5:35:18.0	-5:16:13	214	0.86	14.93	0.0	3	430	...	X
-	-	...	...	967	9224	5:35:18.4	-5:24:27	78	0.42	15.16	2.4	155	70	M2.5	X
592	99	...	...	974	592	5:35:18.5	-5:18:21	285	0.61	14.37	4.0	6	304	M2.5	PX
597	0	...	...	994	597	5:35:18.8	-5:14:46	307	0.17	14.02	0.1	4	519	...	XHV
-	-	...	...	998	9239	5:35:18.8	-5:22:23	314	0.20	17.54	0.3	31	70	...	X
-	-	...	...	1061	5066	5:35:20.0	-5:18:47	71	0.22	17.31	0.1	11	281	M9	OX00
638	99	...	...	1077	638	5:35:20.0	-5:29:12	354	1.01	17.03	3.2	171	353	...	PXV

TABLE 1—*Continued*

JW	%	Par	GCVS	COUP	H97	RA <sub>2000</sub>	DEC <sub>2000</sub>	PA	SEP ["]	m <sub>I</sub>	Δm <sub>Hα</sub> <sup>1</sup>	PA <sub>OriC</sub>	OriC	SpT <sup>2</sup>	Memb. <sup>3</sup>
681	99	...	V1524	...	681a	5:35:21.4	-5:23:45	232	1.09	16.39	0.9	107	77	K7	PX0V
687	54	...	...	1158	687a	5:35:21.7	-5:21:47	231	0.49	14.66	2.1	39	124	...	XV
709	99	1994	...	1202	709	5:35:22.2	-5:26:37	309	0.22	12.92	0.5	156	213	M0.5	PX
722	98	...	...	1208	722	5:35:22.3	-5:33:56	216	0.36	14.51	0.2	172	639	M4.5	PX
727	99	...	V1528	1233	727	5:35:22.8	-5:31:37	285	0.73	13.87	4.7	169	503	M2	PXHV
748	99	...	...	1279	748a	5:35:24.1	-5:21:33	277	0.35	14.77	2.0	46	159	M3	PXV
767	99	...	...	1316	767	5:35:25.2	-5:15:36	75	1.13	13.89	>4.1	16	485	M2.5	PXV
776	99	...	V496	1328	776a	5:35:25.4	-5:21:52	73	0.50	14.20	1.8	56	162	...	PXV
777	80	...	...	1327	777	5:35:25.5	-5:21:36	347	1.19	15.15	1.2	52	173	K6	X
783	95	...	...	...	783	5:35:25.5	-5:34:03	283	0.40	14.17	0.8	168	656	...	PX
797	99	...	...	1363	797	5:35:26.6	-5:17:53	323	1.42	16.30	2.8	25	363	...	PX
-	-	...	...	1425	3042	5:35:29.5	-5:18:46	329	0.23	16.06	2.6	35	338	...	XV
841	99	...	...	...	841	5:35:30.0	-5:12:28	16	0.41	14.41	0.1	17	686	M4	PHV
867	99	2075	...	1463	867	5:35:31.3	-5:18:56	212	0.29	12.19	>0.3	40	347	K8	PXHV
884	99	...	...	...	884	5:35:32.4	-5:14:25	287	1.32	14.91	2.8	24	589	...	P
893	99	...	...	...	893	5:35:33.2	-5:14:11	208	0.15	14.07	0.0	24	606	...	PV
906	99	...	...	...	906	5:35:34.7	-5:34:38	293	1.39	14.17	2.7	158	728	M3	PV
924	99	...	...	...	924	5:35:36.5	-5:34:19	73	1.04	16.63	1.3	156	722	...	P
945	99	2149	...	...	945	5:35:40.2	-5:17:29	46	1.41	12.51	3.6	45	501	B6	P

- a - Prosser et al. (1994)
- b - Padgett et al. (1997)
- c - Simon et al. (1999)
- d - Koehler et al. (2006)
- e - Getman et al. (2005)
- f - Lucas et al. (2005)

<sup>1</sup>The symbol > indicates that the primary is saturated (sometimes both stars), thus Δm is only an approximation

<sup>2</sup>Spectral types obtained at SIMBAD

<sup>3</sup>Membership criteria used: P - proper motion catalog by Jones & Walker (1988) with probability ≥ 93%, X - COUP source by Getman et al. (2005), H - Hα emission (Pettersson et al., in prep.), V - variability noted by the General Catalog of Variable Stars

TABLE 2  
OTHER BINARIES WITH ANGULAR SEPARATIONS <1''5 TOWARD THE ONC.

JW	%	Par	GCVS	COUP	H97	RA <sub>2000</sub>	DEC <sub>2000</sub>	PA	SEP ["]	m <sub>I</sub>	Δm <sub>Hα</sub>	PA <sub>OriC</sub>	OriC	SpT*	Memb.
553	99	1911	V1510	899	553a	5:35:17.6	-5:22:57	113	0.36	12.41	1.4	34	31	K3.5	PXV
596	99	1927	AF	986	596	5:35:18.7	-5:23:14	78	0.30	13.06	2.2	75	34	K3.5	PXV
...	...	...	...	1085	3075	5:35:20.2	-5:23:09	104	0.21	...	0.4	76	57	...	X
182	48	...	...	127	182	5:34:58.0	-5:29:41	77	0.11	16.56	0.2	216	467	...	X
290	99	...	...	266	290	5:35:06.4	-5:27:05	84	0.11	15.48	1.3	214	268	...	PX
-	-	...	...	1195	3034	5:35:22.3	-5:18:09	227	0.11	15.67	0.8	15	326	...	X
...	...	1423	...	...	3114	5:34:19.5	-5:27:12	168	0.56	10.52	0.1	255	881	G5	...
58	0	...	...	...	58	5:34:41.8	-5:34:30	282	1.43	16.13	2.2	218	844	...	...
61	46	...	...	...	61	5:34:42.7	-5:28:37	153	0.45	13.52	0.9	238	594	...	...
...	...	...	...	...	...	5:34:45.8	-5:30:58	324	0.46	...	0.1	225	645	...	...
...	...	...	...	...	10343	5:35:01.4	-5:24:13	292	0.28	...	0.6	257	231	...	...
...	...	...	...	...	9221	5:35:18.3	-5:24:39	96	0.67	16.72	2.2	160	81	...	...
...	...	...	...	...	...	5:35:30.0	-5:34:31	237	1.29	...	0.3	163	699	...	...

- a - Prosser et al. (1994)
- 1 - Binaries with angular separation <0''4 inside the exclusion zone
- 2 - Binaries with angular separation <0''15 outside the exclusion zone
- 3 - Binaries with angular separation <1''5 outside the exclusion zone but with no evidence of ONC membership

\*Spectral types obtained at SIMBAD



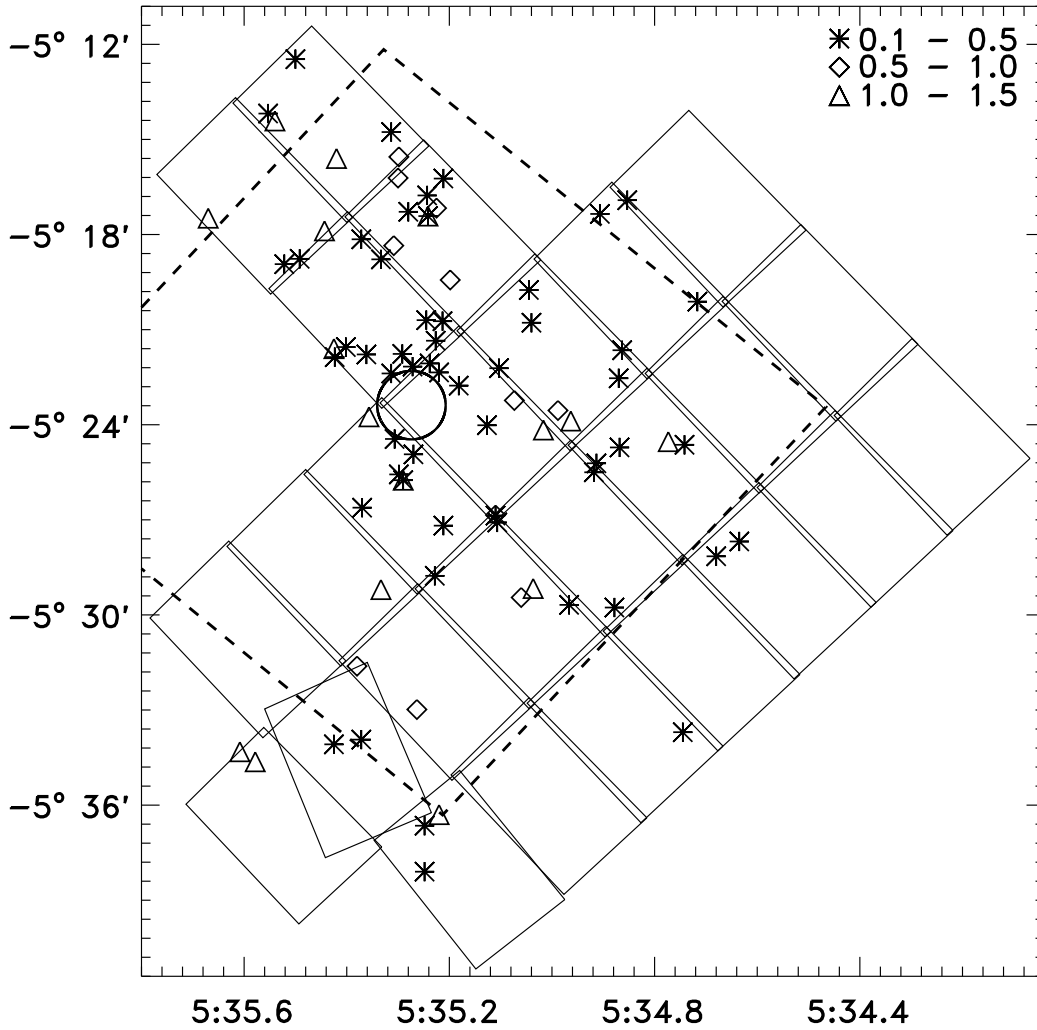


Fig. 1.— Distribution of HST images across the ONC. The  $60''$  exclusion zone centered on  $\theta^1$  Ori C is marked by a circle, and the boundaries of the COUP survey is indicated with dashed lines. Binaries in three different separation ranges are marked by different symbols (asterisks:  $0''.1 - 0''.5$ , diamonds:  $0''.5 - 1''.0$ , triangles:  $1''.0 - 1''.5$ ). Coordinates are equinox 2000.

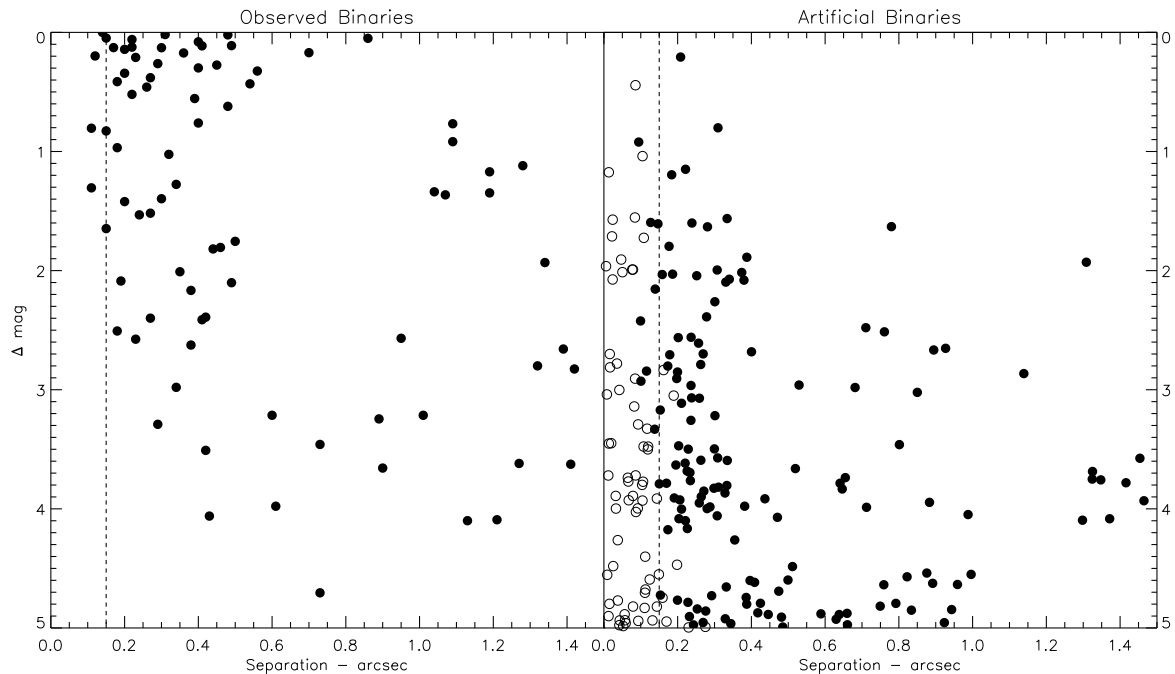


Fig. 2.— Two plots showing  $\Delta m$  vs. binary separation in arcseconds. The left panel shows the actual binaries observed, while the right panel shows “observations” of actual stellar images to which artificial companions were added with random separations, position angles, and  $\Delta m$ . Filled circles indicate those companions we could detect, and empty circles those we failed to see. The vertical dashed line indicates the  $0''.15$  limit we adopted as our completeness limit.

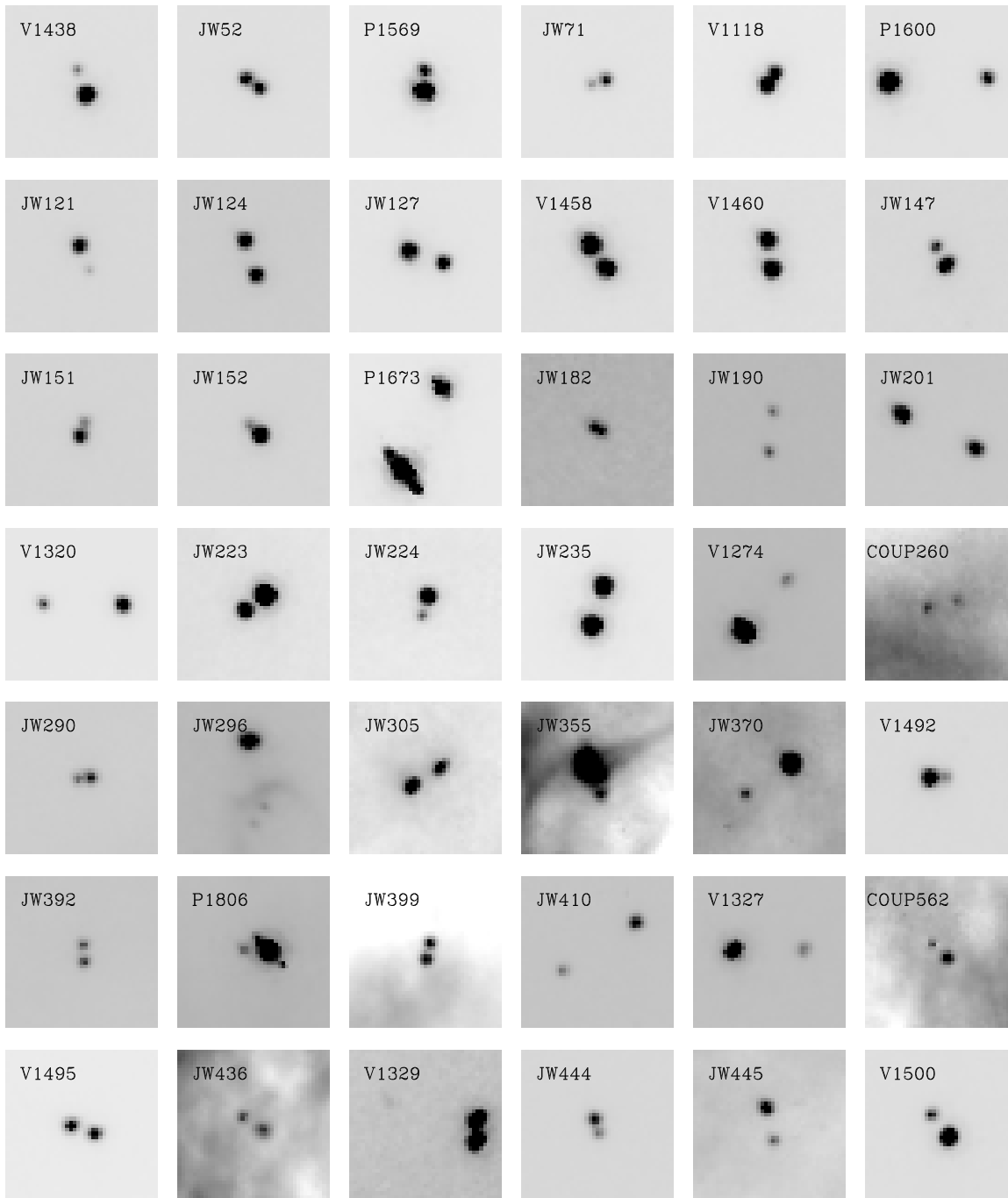


Fig. 3.— All binaries identified among the ONC members. Each stamp is  $2''$  wide, and in each panel, north is up and east is to the left.

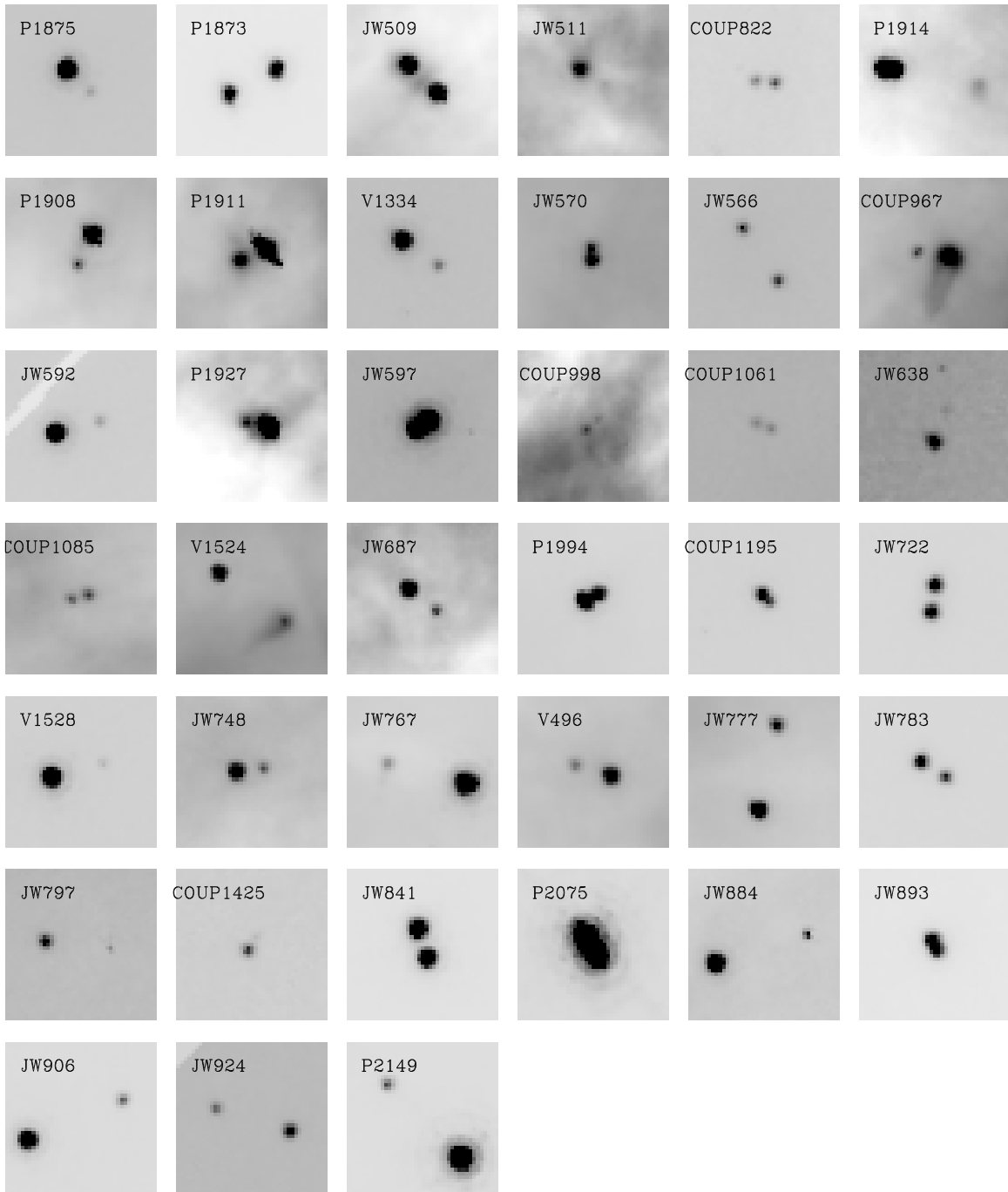


Fig. 3.— continued

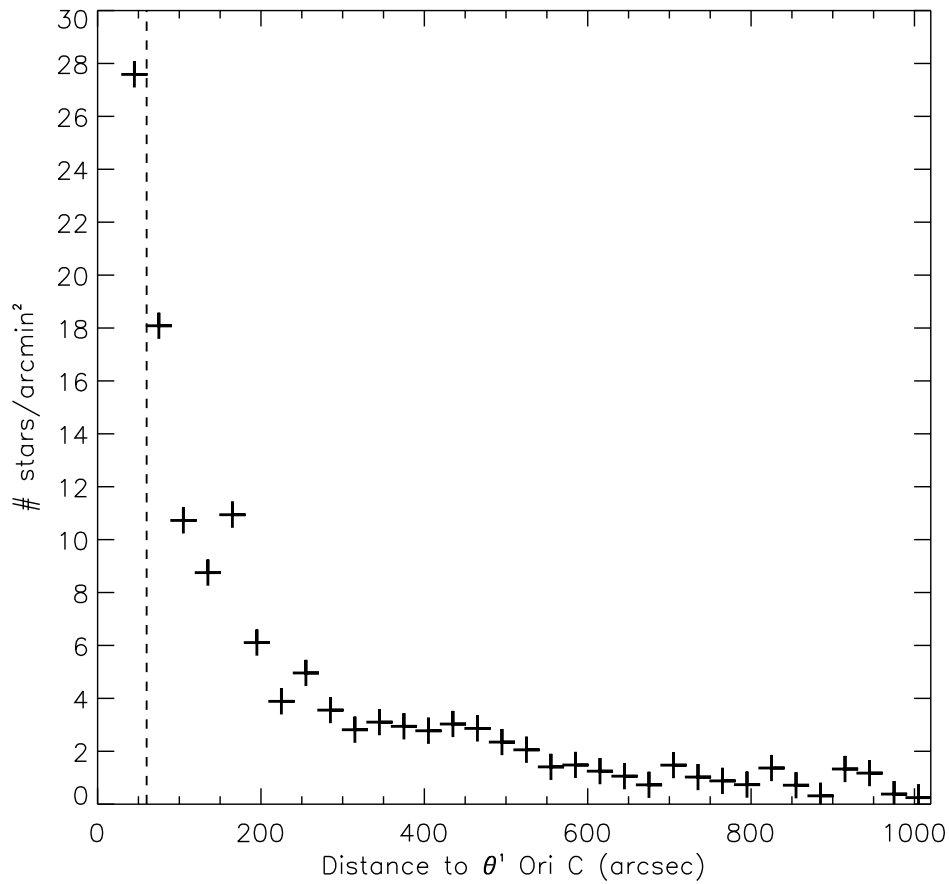


Fig. 4.— The surface density of stars in M42 as a function of distance from  $\theta^1$  Ori C. Measurements have been done in  $30''$  wide annuli on our ACS images. The vertical dotted line indicates the  $60''$  exclusion zone inside which we did not attempt to identify visual binaries due to the high density of stars.

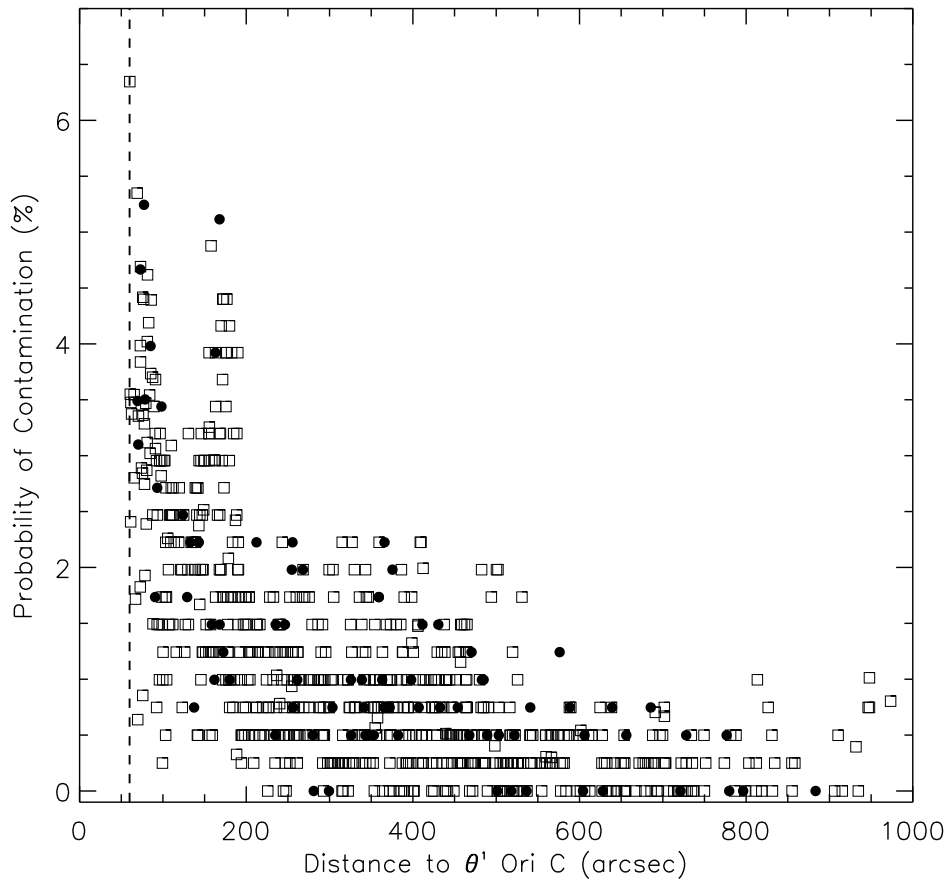


Fig. 5.— The probability that a star would have another star as a line-of-sight association within a separation of  $1''.5$  for all 781 ONC members in our list and as a function of distance from  $\theta^1$  Ori C. White squares are single stars and black circles are confirmed binaries. The peak around  $180''$  is due to a subclustering of stars.

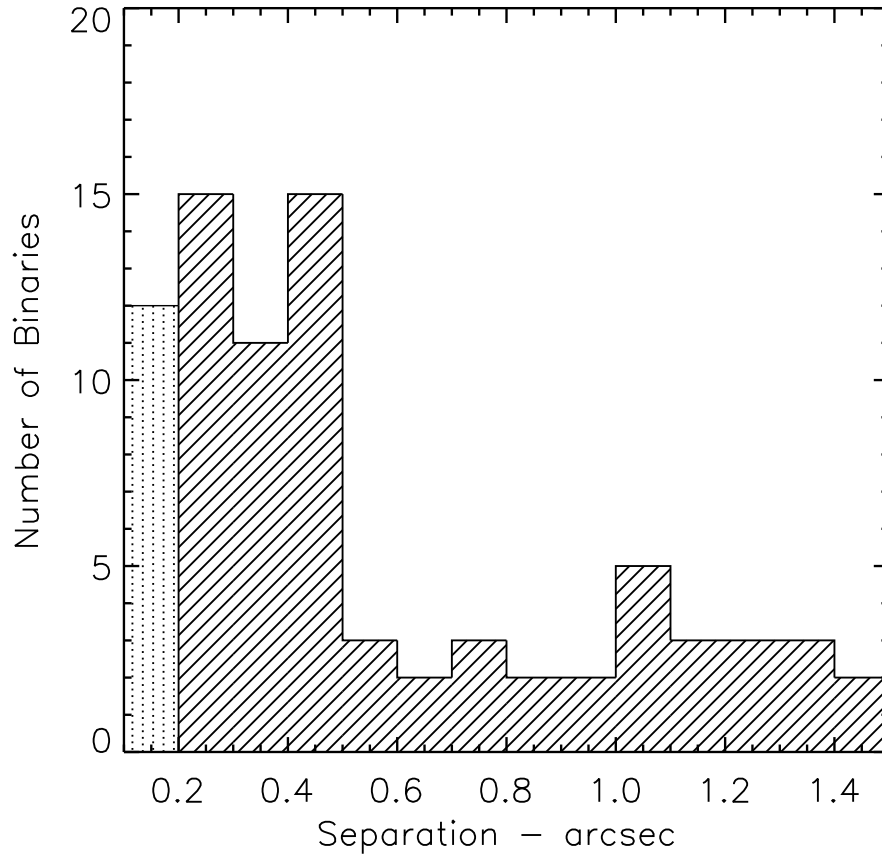


Fig. 6.— Histogram of binary separations as function of angular separation in steps of  $0''.1$ . The number of binaries in the innermost bin with separations less than  $0''.1$  is incomplete. There is a dramatic decrease in the number of binaries when the separation increases beyond  $0''.5$ .

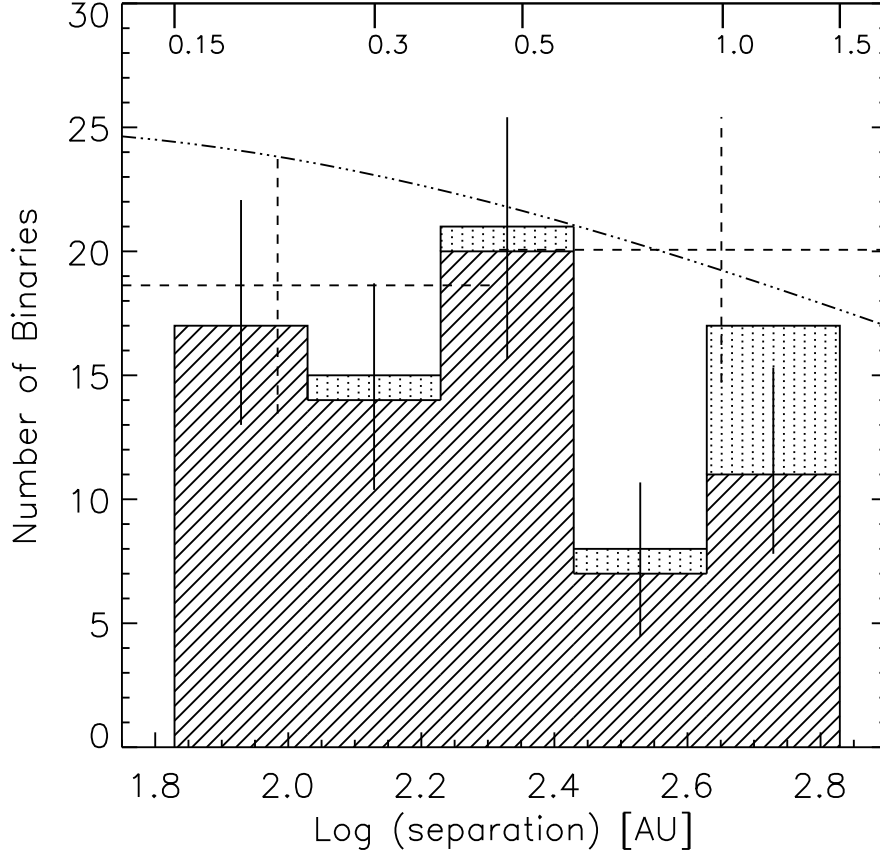


Fig. 7.— Logarithmic separation distribution function of ONC binaries compared to the distribution of field binaries from Duquennoy & Mayor (1991) across the separation range from  $0''.15$  to  $1''.5$ . The actual data from Duquennoy & Mayor within our observed range are marked by two dashed crosses and the Gaussian distribution that they fit to their complete data set is indicated by the dot-dashed curve. The parts of the columns that are dotted indicate the 9 binaries that we calculate are due to line-of-sight associations. The axis on top indicates separations in arcseconds at the distance of the ONC. A scaling was done to correct for the fact that Duquennoy & Mayor has a smaller sample size (164 vs. 781) and a larger bin width (0.667 vs. 0.2 in  $\log(\text{AU})$ ), hence a factor of  $(781/164) \times (0.2/0.667) = 1.43$  was applied to compare the distributions directly.



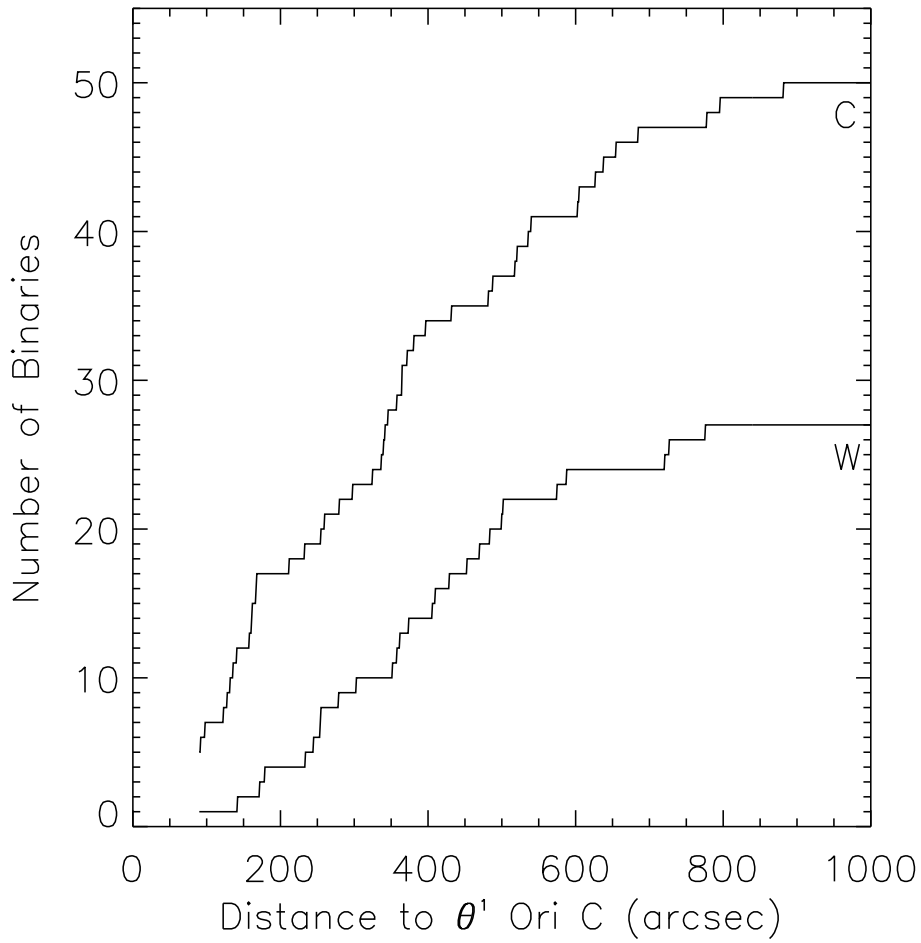


Fig. 8.— Cumulative distributions of close ( $0''.15$  -  $0''.5$ ) and wide ( $0''.5$  -  $1''.5$ ) binaries in the ONC as a function of distance from  $\theta^1$  Ori C.

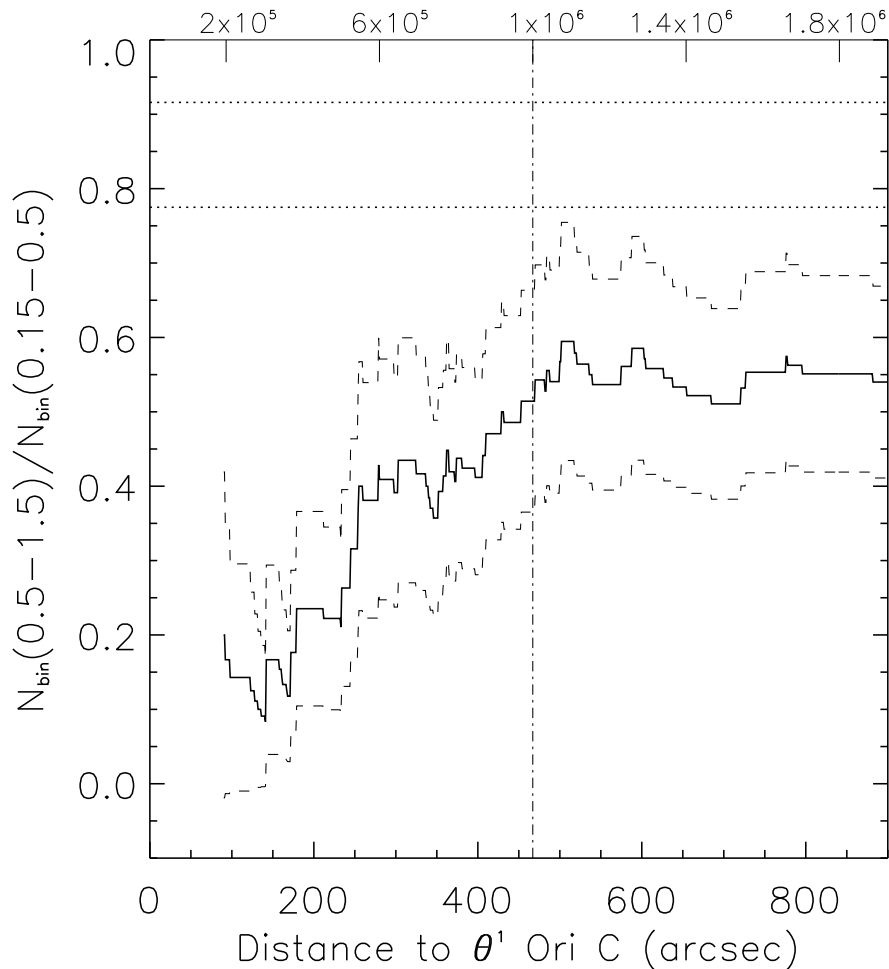


Fig. 9.— The ratio of wide ( $0''.5 - 1''.5$ ) to close ( $0''.15 - 0''.5$ ) binaries in the ONC as a function of distance to  $\theta^1$  Ori C. The figure shows this ratio for all binaries from the  $60''$  exclusion zone and out to a given distance. The last value at around  $900''$  thus represents the value of *all* binaries within the above ranges in the ONC outside the exclusion zone. The dashed lines indicate the errors on the numbers. The dotted horizontal lines represent the same ratio from the Duquennoy & Mayor (1991) field binary study, with the lower being from the Gaussian fit, and the upper from their actual data points. The upper scale indicates the crossing time in years, assuming a mean one-dimensional velocity dispersion of 2 km/sec. The vertical line indicates the distance where the ratio becomes flat, suggesting an age for the ONC of about  $10^6$  yr.

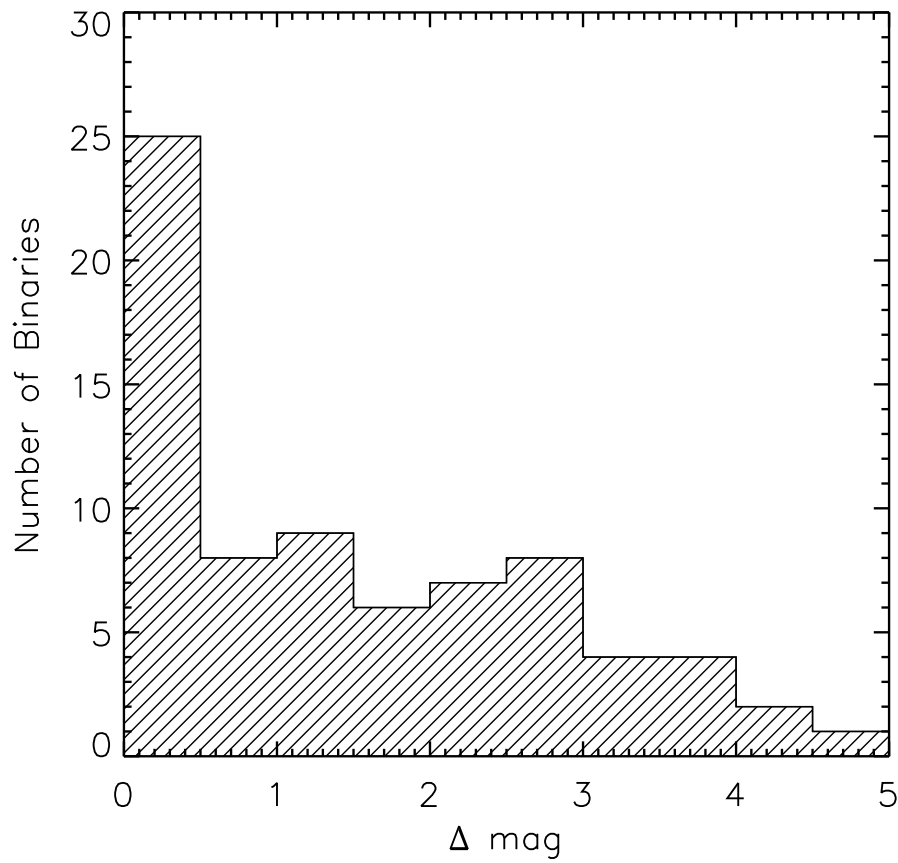


Fig. 10.— Luminosity ratio of the binary population, based on the  $H\alpha$  fluxes of primaries and secondaries. All stars with separations between  $0''.1$  and  $1''.5$  from Tables 1 and 2 are plotted, except if they are saturated.